Accepted Manuscript

Comparison to mechanical properties of epoxy nanocomposites reinforced by functionalized carbon nanotubes and graphene nanoplatelets

Jaemin Cha, Joonhui Kim, Seongwoo Ryu, Soon H. Hong

PII: S1359-8368(18)32319-9

DOI: https://doi.org/10.1016/j.compositesb.2018.11.011

Reference: JCOMB 6196

To appear in: *Composites Part B*

Received Date: 26 July 2018

Revised Date: 30 October 2018

Accepted Date: 1 November 2018

Please cite this article as: Cha J, Kim J, Ryu S, Hong SH, Comparison to mechanical properties of epoxy nanocomposites reinforced by functionalized carbon nanotubes and graphene nanoplatelets, *Composites Part B* (2018), doi: https://doi.org/10.1016/j.compositesb.2018.11.011.

Comparison to Mechanical Properties of Epoxy Nanocomposites Reinforced by Functionalized Carbon Nanotubes and Graphene Nanoplatelets

Jaemin Cha[1], Joonhui Kim[1], Seongwoo Ryu[2, †] and Soon H. Hong[1, *]

[1]Department of Material Science and Engineering, Korea Advanced Institute of Science and Technology (KAIST), 291 Daehak-ro, Yuseong-gu, Daejeon, 34141, Republic of Korea

[2]Department of polymer Engineering, College of Engineering, University of Suwon, 17 Wauan-gil, Bongdam-eup, Hwaseong-si, Gyeonggi-do, 18323, Republic of Korea

Abstract

Low-dimension carbon nanomaterials, such as carbon nanotubes (CNTs) and graphene nanoplatelets (GNPs), are effective mechanical reinforcements in polymer composites. Epoxy matrix composites were fabricated by functionalizing CNT and GNP nanofillers using melamine and nondestructive ball milling. This noncovalent functionalization prevents agglomeration of nanofiller and produces direct C-N bonds with the epoxy matrix. Compared to pristine CNTs and GNPs/epoxy nanocomposites, melamine-functionalized CNT (M-CNT)/epoxy and melamine-functionalized GNP (M-GNP)/epoxy nanocomposites exhibited considerably higher tensile strengths and fracture toughness (single edge notch bending, SENB). At 2 wt%, both M-CNT/epoxy and M-GNP/epoxy nanocomposites exhibited enhanced Young's modulus values (M-CNT: 64 % and M-GNP: 71%) and ultimate tensile

*Corresponding author. Tel: (+82) 42 350 3327, E-mail: shhong@kaist.ac.kr (Soon H. Hong)
†Co-corresponding author. Tel: (+82) 55 350 3812, E-mail: ryu@suwon.ac.kr (Seongwoo Ryu)

strengths (M- CNT: 22 % and M-GNP: 23%). Fracture toughness increased by 95% with the 2 wt% M-CNT/epoxy and by 124% with the 2 wt% M-GNP/epoxy nanocomposite. The reinforcing effects of the two-dimensional M-GNPs were greater than those of the one-dimensional M-CNTs due to differences in pull-out mechanisms and bridging effects. Crack propagation in the nanocomposites, as it relates to fracture toughness, was also investigated.

Key Words: A. Polymer nanocomposites; B. Carbon Nanotubes; C. Graphene Nanoplatelets; D. Mechanical Properties

1. Introduction

Engineering polymers are used in a wide number of applications due to their high flexibility, processability, and relatively low cost. Among them, epoxy resins have received enormous interest from scientists for use in composite materials. Uncured epoxy resins have poor mechanical, chemical, and thermal properties. Reacting an epoxy resin with a suitable curing agent results in three-dimensional (3-D), cross-linked, thermoset structures with a high modulus, high failure strength, and high bond strength [1-3].

However, higher cross-link densities can contribute to low absolute strength and poor fracture toughness, limiting epoxy composite use in applications involving mechanical components [4]. Various types of reinforcements have been developed to improve the mechanical properties of epoxy composites [5-8].

Among these, nanofillers, including low-dimensional carbon nanomaterials, have attracted considerable attention due to their low density, and excellent mechanical, electrical, and thermal properties in epoxy matrix composites [9-11]. Typical examples include one-

dimensional (1-D) carbon nanotubes (CNTs), two-dimensional (2-D) graphene nanoplatelets (GNPs), and 3-D graphite [11]. The application of nanofillers has a significant impact on the interfacial load transfer levels of multifunctional nanocomposite materials. The interfacial area between a nanofiller and a polymer matrix varies according to the dimension and structure of the nanofillers[12-13]. For example, CNTs can interact a with polymer matrix through 1-D linear contact. In contrast, layered 2-D nanofillers like GNPs boast larger contact areas with polymer chains, leading to higher-performing composites [14-15]. Due to their flat surfaces and lateral dimensions, GNPs exhibit larger aspect ratios and greater specific surface areas than CNTs. These characteristics play an important role in enhancing the mechanical properties of polymer composites [16-18].

However, poor dispersibility and the low interfacial strength of nanofillers in polymer matrices have limited their applications. Furthermore, van der Waals forces between low-dimensional carbon nanomaterials can lead to agglomeration and, consequently, difficulties in obtaining homogeneous dispersion in a polymer matrix [19].

Enhancements in dispersibility and interfacial strength can be achieved by functionalization. Functionalizing low-dimensional carbon nanomaterials such as CNTs and GNPs, either covalently or noncovalently, is an effective means of preventing nanofiller agglomeration and improving load transfer at the nanofiller/matrix interface [20-23]. Covalent functionalization is usually characterized by oxidation of CNTs or GNPs in an acid to attach carboxylic or hydroxyl groups at end-caps or defect sites [24]. This technique can dramatically improve the interfacial interactions between a nanofiller and a polymer matrix via direct chemical bonding [25]. Noncovalent functionalization is an alternative method for modifying the surface of CNTs or GNPs [26-27] and is characterized by interactions between

delocalized π-bonds on the surface of the nanofiller, due to sp^2 hybridization [28], and hexagonal ring structures on the functionalizing moieties. The advantage of noncovalent functionalization is that it neither destroys the surface of the nanomaterial nor affects its final structure. Therefore, noncovalent functionalization is more attractive than covalent functionalization for maintaining the pristine structures and native properties of CNTs and GNPs [29-30]. In particular, the incorporation of amino-functionalized CNTs and GNPs provides huge improvements to the interfacial strengths of epoxy matrix composites. Direct C-N covalent bonds can form between the epoxy matrix and amino groups (NH_2) on the nanofiller through the ring-opening reaction of epoxide (C-O-C) groups [31-32].

In this work, we fabricated an epoxy matrix nanocomposite by functionalizing 1-D CNTs and 2-D GNPs with melamine, generating melamine-CNTs (M-CNTs) and melamine-GNPs (M-GNPs), using a nondestructive ball milling process. Melamine has a conjugated structure containing sp^2-hybridized carbon, making it suitable for both noncovalent functionalization through π-π interactions, and covalent functionalization through the chemical bonding of amine groups to the epoxy matrix. The fracture and strength mechanics of the resulting composites were analyzed by determining their microstructure, tensile strength, Young's modulus value, and fracture toughness.

2. Experimental procedure

2.1 Materials

The materials used in this study were epoxy resin, melamine-functionalized multiwall carbon nanotubes (M-CNTs), and GNPs (M-GNPs). MWCNTs (2.1±0.050g/cm^3, Hanwha

Chemical, Korea) were produced by combustion chemical vapor deposition (CCVD) yielding tubes with diameters from 10 to 20 nm and more than 5 μm in length. GNPs (2.1±0.050g/cm^3, XG-Science, Lansing, MI, USA) were used as reinforcements. The GNPs ranged in size from 2 to 15 μm with a thickness of about 50 nm (25 layers), as shown in Fig. S3. Melamine, which has hexagonal rings suitable for π-π interactions with both CNTs and GNPs, was acquired from Aldrich. Epoxy resin MY 0510 (triglycidyl p-aminophenol, TGAP; Hunstman, Switzerland) was selected due to its low viscosity and extensive industrial applications. A low-viscosity matrix is more conducive to the uniform dispersion of additives. The resin curing agent was diaminodiphenylsulfone (DDS) and was mixed at a 100:30 ratio (MY 0510:DDS) to form the matrix material.

2.2 Preparation of Melamine-CNTs and Melamine-GNPs

Melamine 500 mg was dissolved in N,N-dimethylforamide 80ml (DMF; Junsei) by stirring for 10 min. This solution was then sonicated for 1 h with 500 mg of CNTs or GNPs. For functionalization, the resulting mixture was ball-milled in a polypropylene (PP) bottle at a ball-to-product weight ratio of 1000:1 and a rotation speed of 200 rpm for 24 h (Fig. 1a). After ball milling, the carbon nanomaterials and melamine were bound by π-π interactions as shown in Fig. 1b. The hexagonal rings of melamine were adsorbed onto the surface of CNTs and GNPs. After adsorption, the solution was filtered under vacuum for 30 min. The resulting black solid was dried at room temperature under reduced pressure.

2.3 Preparation of M-CNT/epoxy and M-GNP/epoxy nanocomposite resins

Functionalized CNTs and GNPs were mixed into the epoxy resin using a planetary centrifugal mixer at 2000 rpm for 2 h. As shown in Fig. 1c, this mixer employs a mechanism wherein the container holding the material revolves clockwise (revolution) and the container itself rotates counter-clockwise (rotation). To assess the effects of functionalization, epoxy nanocomposites reinforced with pristine CNTs and GNPs were also prepared. Homogeneous mixtures of epoxy and reinforcement were cast in dog bone-shaped and single-edge notch three-point bending (SENB) stainless steel molds and degassed at 95°C for 6 h under vacuum. Digital photographs and the dimensions of the specimens are shown in Fig. S1. Finally, specimen curing was conducted at 180°C for 6 h. In all cases, 2 wt% reinforcements were added to the epoxy matrix.

2.4 Specimen characterizations

Microstructural observations of nanocomposites were performed with a scanning electron microscope (SEM, Hitachi S-480). Fracture surfaces of specimens following mechanical tests were used to evaluate the degree of dispersion of CNTs or GNPs. Raman spectroscopy was performed with a Raman spectrometer from LabRAM. Thermo-gravimetric analyses (TGA) were performed with a TGA 92-18 device (Setaram) from 50 to 1000°C at a heating rate of 10°C/min in air. The tensile properties of epoxy nanocomposites were measured using a universal testing machine (INSTRON 8848 microtester) according to ASTM D638, with a crosshead speed of 0.75 mm/min at room temperature. Dog bone-shaped specimens, with a length of 41.25 mm and a width of 4.75 mm, were used after surface polishing. The toughness properties of the epoxy composites were examined using a larger test machine (INSTRON 5583) and performed according to ASTM D5045-99. SENB specimens were

55.88 mm long (l), with a thickness (B) of 6.35 mm and a width (W) of 12.7 mm. A natural crack was created by tapping the specimen with a razor blade placed in the notch. Crack length (a) was selected such that $0.45 < a/W < 0.55$. All a/W ratios were adjusted to approximately 0.5. The crosshead speed was 2 mm/min at room temperature. Five or seven specimens were tested for each configuration.

3. Results and discussion

3.1 Characterization of functionalized CNTs and GNPs

Resonance Raman spectra were acquired from 500 to 3000 cm^{-1}; π-π interactions occurred between melamine and the CNTs and GNPs, as shown in Fig. 2. Four types of 2D bands, corresponding to pristine CNTs, M-CNTs, pristine GNPs, and M-GNPs, were observed. In most cases, bilayer and few-layer graphene can up-shift the 2D band compared with that of single-layer graphene [33-35]. As the bending characteristics in carbon materials such as π-π interactions, doping, sp-bonding, etc., the 2D band was shifted comparing with pristine CNTs and GNPs. Therefore, of the spectra in Fig. 2, the Raman spectrum of pristine GNPs shows the highest frequency 2D band (2727 cm^{-1}) due to its multiple layers of graphene. After functionalization, the bending characteristics was changed, resulting in a 20 cm^{-1} down-shift (2707 cm^{-1}). Similarly, the M-CNTs up-shifts the 2D band relative to that of pristine CNTs. The 2D band of M-CNTs was at 2690 cm^{-1}, whereas that of pristine CNTs was at 2683 cm^{-1}. This suggests that CNTs and melamine bond via π-π interactions.

TGA analyses provided evidence of noncovalent functionalization of CNTs and GNPs with melamine. Fig. 3 shows thermograms of melamine, pristine CNTs, M-CNTs, pristine GNPs,

and M-GNPs in air. Pristine CNTs showed a high thermal stability and did not decompose, even at temperatures above 1000°C. Melamine only showed signs of decomposition above 250°C. The thermal degradation of M-CNTs was qualitatively similar to the sum of the melamine and CNT thermograms. The quantity of functionalized melamine was estimated as approximately 46 wt%. Pristine GNPs exhibited a lower thermal stability than CNTs, but the degradation behavior of M-GNPs was also similar to the sum of melamine and pristine GNP thermograms. The quantity of melamine was about 44 wt%.

3.2 Mechanical properties of M-CNT/epoxy and M-GNP/epoxy nanocomposites

Representative tensile properties of pure epoxy, pristine CNT/epoxy, M-CNT/epoxy, pristine GNP/epoxy, and M-GNP/epoxy nanocomposites are shown in Fig. 4. Fig. S2 presents strain–stress curves obtained from all of the nanocomposites.

Young's modulus and ultimate tensile strength of pure epoxy were 3.35 GPa (n = 7) and 86.04 MPa (n = 7), respectively. The addition of either M-CNTs or M-GNPs significantly enhanced composite strength. With the addition of M-CNTs, Young's modulus and ultimate tensile strength increased by 64% and 22% to 5.53 GPa (n = 7) and 105.01 MPa (n = 7), respectively. These enhancements were even more significant with the addition of M-GNPs, which showed a 71% increase in Young's modulus to 5.76 GPa (n = 7) and an increase of 23% in tensile strength to 105.91 MPa (n = 6). The reinforcing effects of 2-D M-GNP/epoxy were stronger than those of 1-D M-GNP/epoxy due to the larger aspect ratio and specific surface area of the former.

However, measurements of the mechanical properties of pristine CNT/epoxy and

GNP/epoxy composites showed slight increases in Young's modulus, but with concurrent decreases in tensile strength. These results demonstrate that noncovalent functionalization of melamine can enhance the reinforcement properties of CNTs and GNPs in epoxy nanocomposites, presumably by improving the dispersion of CNTs and GNPs. Melamine interacts with CNTs and GNPs via π-π interactions and inhibits both the agglomeration of CNTs and the restacking of GNPs. In addition, the amino groups ($-NH_2$) of melamine provide covalent handles for strong interactions with the epoxy system. These interactions result in enhanced load transfer across the epoxy/nanocomposite interface.

3.3 Microstructures of M-CNT/epoxy and M-GNP/epoxy nanocomposites

SEM images obtained from the fracture surfaces of epoxy nanocomposites following tensile tests are shown in Fig. 5. Figs 5a and b show that pristine CNTs and GNPs had agglomerated in the epoxy matrix, which could be divided into additive-rich and additive-poor regions. In contrast, M-CNTs and M-GNPs dispersed homogenously throughout the epoxy matrix (Figs 5c and d). The addition of melamine prevented the agglomeration of CNTs and GNPs. In composites containing pristine CNTs and GNPs, load transfer between the additives and the epoxy matrix was inhibited. These points acted as defect sites in the epoxy nanocomposites.

3.4 Fracture toughness properties of M-CNT/epoxy and M-GNP/epoxy nanocomposites

The use of nanofiller as a structural element in an epoxy matrix is based largely on anticipated enhancements to fracture toughness. Fig. 6 shows the results of fracture toughness

measurements on M-GNP/epoxy and M-GNP/epoxy nanocomposites.

Fracture toughness, K_{Ic}, was calculated using the following relationship in ASTM D5045-99:

$$K_Q = \left(\frac{P_Q}{BW^{1/2}}\right) f(x), \quad W=2B \tag{1}$$

$$f(x) = 6x^{1/2}\frac{[1.99 - x(1-x)(2.15 - 3.93x + 2.7x^2)]}{(1+2x)(1-x)^{3/2}}, \tag{2}$$

where K_Q is the provisional fracture toughness, f is the shape factor, P_Q is the peak load, B is the specimen thickness, W is the specimen width, and a is the crack length.

Both the M-GNP/epoxy and M-GNP/epoxy nanocomposites had significantly higher fracture toughness values than pure epoxy (K_{Ic} = 1.01 MPa*m$^{1/2}$, n = 5). The K_{Ic} values of M-CNT and M-GNP/epoxy were 1.95 MPa*m$^{1/2}$ (n = 6) and 2.24 MPa*m$^{1/2}$ (n = 6), respectively. M-CNT/epoxy specimens exhibited a toughening effect as high as 95% and the M-GNP/epoxy specimens showed a 124% increase in fracture toughness, as illustrated in Fig. 6. The difference in relative enhancement between these two samples is caused by different pull-out mechanisms and bridging effects.

The fracture toughness of nanocomposites incorporating pristine CNTs and GNPs was approximately 1.46 MPa*m$^{1/2}$ (n = 6), which corresponds to a 47% increase over that of epoxy alone. Agglomerated CNTs and GNPs acted as obstacles to crack propagation.

M-CNTs and M-GNPs composites exhibited improved nanofiller dispersion and enhanced interfacial adhesion, providing a large effective interfacial area. Melamine appears in domains on the surfaces of both CNTs and GNPs, with the nanofiller being locally bonded to

the epoxy matrix. Therefore, the observed enhancements in fracture toughness may be attributed to interfacial bonding between the nanofillers and the matrix.

Due to their agglomeration in the epoxy matrix, pristine CNTs and GNPs were unable to arrange in such a way as to prevent crack propagation (Figs 7a and b). Some bridging structures arose, but they were easily broken or misshapen. As a result, cracks were transferred to the interface between misshapen bridges and the epoxy matrix.

With M-CNTs, the dominant toughening mechanisms are pull-out and crack bridging. As a crack opens, energy is dissipated by the frictional pull-out of CNTs from the epoxy matrix. This slows crack propagation. Fracture toughness may also be enhanced by CNTs that bridge the crack and hinder crack opening. The micrographs in Fig. 7c show both pull-out and crack bridging of M-CNTs. Similar phenomena with M-GNPs can be seen in Fig. 7d.

Similar toughening mechanisms were observed with both M-GNP to M-CNT nanocomposites. Frictional pull-out of GNPs is considered a primary source of fracture toughness given the strong interfacial adhesion between GNPs and the epoxy matrix. Many studies have investigated pull-out energies and derived mathematical expressions for fiber-reinforced polymer matrices [36]. However, few studies have examined 2-D nanomaterial reinforcements in polymer nanocomposites. According to Lau, Epull-out, or the pull-out energy of nanotubes, can be calculated using simple shear lag theory:

$$E_{pull-out} = \int_0^{L_{tube}} 2\pi r(L_{tube} - x)\tau_i dx = \tau_i \pi r {L_{tube}}^2 \quad (3)$$

Where τ_i is the interfacial shear stress, L_{tube} is the nanotube length, r is the nanotube radius, and x is the displacement of the nanotube.

To further simplify the calculation of pull-out energy in M-GNP/epoxy nanocomposites,

we modified the equation to consider GNPs in place of nanotube reinforcements. We assumed that a GNP is a regular hexagon with side length *w* and thickness *t*. In addition, Lnanoplatelet is the diagonal length of the nanoplatelet. A schematic diagram of the pull-out behavior is illustrated in Figs 7e and f. The pull-out energy of GNP nanoplatelets is denoted as follows:

$$E_{pull-out} = \int_0^{L_{nanoplatelet}} (\frac{3\sqrt{3}}{2} w + 2t)(L_{nanoplatelet} - x)\tau_i dx \quad (4)$$

Assuming that the nanoplatelets are very thin and hexagon-shaped, then $t \ll w$, and $L_{nanoplatelet} = 2w$.

$$E_{pull-out} \cong 3\sqrt{3}\tau_i w^3 \quad (5)$$

We further assumed interfacial stress, τ_i, to be constant, although it scales with bond stress and changes during the pull-out process, because CNTs and GNPs contain the same functional groups. The pull-out direction of a nanoplatelet was considered to be solely longitudinal, and we disregarded the flexibility of CNTs and GNPs. In this study, the radius of a CNT, *r*, was 7.5±2.5nm and L_{tube} was 7.5±2.5μm. Furthermore, as shown in Fig. S3, the length of one side of a GNP was 5.92±0.45μm. Accordingly, the calculated pull-out energy of a GNP was larger than that of a CNT. Moreover, the large aspect ratio of a hexagonal nanoplatelet has a large impact on its pull-out energy.

4. Conclusions

This report described noncovalent functionalization with melamine as a means of improving the mechanical properties of epoxy matrices reinforced with CNTs and GNPs. A

non-destructive ball milling process was used to functionalize CNT and GNP nanofillers with melamine and a planetary centrifugal mixer was used to mix the nanofillers into an epoxy resin. Melamine was bound to the surface of CNTs or GNPs by π-π interactions, which prevented agglomeration of the nanofiller and afforded direct interfacial bonding with the epoxy matrix. Both M-CNT/epoxy and M-GNP/epoxy nanocomposites showed improved mechanical properties over those made with CNT/epoxy and GNP/epoxy nanofillers. The greatest improvements were observed with M-GNP/epoxy, which boasted a 71% enhancement in Young's modulus, a 23% enhancement in ultimate tensile strength, and a 124% enhancement in fracture toughness. These results are due to geometric differences between the nanofillers. 2-D nanoplatelets offer a larger interface than 1-D nanotubes. This provides for greater load transfer between the matrix and the nanofiller, which yields better crack bridging and helps prevent pull-out. As a result, nanocomposites made with epoxy and M-GNPs showed remarkably enhanced mechanical properties. This simple and effective approach to nanocomposite fabrication is applicable to any general polymer matrix and will aid in the development of next-generation lightweight and high-strength materials.

Acknowledgements

This research was supported by Nano Material Technology Development Program through the National Research Foundation of Korea (NRF) funded by the Ministry of Science, ICT and Future Planning (2016M3A7B4905630) and was supported by First Research in Lifetime program through the NRF funded by the Ministry of Education (NRF-2017R1C1B5076552).

Reference

[1] Domun N, Hadavinia H, Zhang T, Sainsbury T, Liaghat GH, Vahid S. Improving the fracture toughness and the strength of epoxy using nanomaterials - a review of the current status. Nanoscale. 2015;7(23):10294-329.

[2] Kinloch AJ. Toughening epoxy adhesives to meet today's challenges. Mrs Bull. 2003;28(6):445-8.

[3] Vietri U, Guadagno L, Raimondo M, Vertuccio L, Lafdi K. Nanofilled epoxy adhesive for structural aeronautic materials. Compos Part B-Eng. 2014;61:73-83.

[4] Kinloch AJ, Lee SH, Taylor AC. Improving the fracture toughness and the cyclic-fatigue resistance of epoxy-polymer blends. Polymer. 2014;55(24):6325-34.

[5] Schueler R, Petermann J, Schulte K, Wentzel HP. Agglomeration and electrical percolation behavior of carbon black dispersed in epoxy resin. J Appl Polym Sci. 1997;63(13):1741-6.

[6] Lan T, Pinnavaia TJ. Clay-Reinforced Epoxy Nanocomposites. Chem Mater. 1994;6(12):2216-9.

[7] Johnsen BB, Kinloch AJ, Mohammed RD, Taylor AC, Sprenger S. Toughening mechanisms of nanoparticle-modified epoxy polymers. Polymer. 2007;48(2):530-41.

[8] Ajayan PM, Schadler LS, Giannaris C, Rubio A. Single-walled carbon nanotube-polymer composites: Strength and weakness. Adv Mater. 2000;12(10):750-+.

[9] Jensen BD, Odegard GM, Kim J-W, Sauti G, Siochi EJ, Wise KE. Simulating the effects

of carbon nanotube continuity and interfacial bonding on composite strength and stiffness. Composites Science and Technology.

[10] Wang AL, Xu H, Liu X, Wang S, Zhou Q, Chen J, et al. High electrochemical performances of solid nano-composite star polymer electrolytes enhanced by different carbon nanomaterials. Composites Science and Technology. 2017;152:68-75.

[11] Choudhary N, Hwang S, Choi W. Carbon Nanomaterials: A Review. In: Bhushan B, Luo D, Schricker SR, Sigmund W, Zauscher S, editors. Handbook of Nanomaterials Properties. Berlin, Heidelberg: Springer Berlin Heidelberg; 2014. p. 709-69.

[12] Chiu YC, Huang CL, Wang C. Rheological and conductivity percolations of syndiotactic polystyrene composites filled with graphene nanosheets and carbon nanotubes: A comparative study. Composites Science and Technology. 2016;134:153-60.

[13] Punetha VD, Rana S, Yoo HJ, Chaurasia A, McLeskey JT, Ramasamy MS, et al. Functionalization of carbon nanomaterials for advanced polymer nanocomposites: A comparison study between CNT and graphene. Prog Polym Sci. 2017;67:1-47.

[14] Bhattacharya M. Polymer Nanocomposites-A Comparison between Carbon Nanotubes, Graphene, and Clay as Nanofillers. Materials. 2016;9(4).

[15] Li B, Dong S, Wu X, Wang CP, Wang XJ, Fang J. Anisotropic thermal property of magnetically oriented carbon nanotube/graphene polymer composites. Composites Science and Technology. 2017;147(Jul):52-61.

[16] Hao B, Ma Q, Yang SD, Mader E, Ma PC. Comparative study on monitoring structural damage in fiber-reinforced polymers using glass fibers with carbon nanotubes and graphene coating. Composites Science and Technology. 2016;129:38-45.

[17] Chatterjee S, Nuesch FA, Chu BTT. Comparing carbon nanotubes and graphene nanoplatelets as reinforcements in polyamide 12 composites. Nanotechnology. 2011;22(27).

[18] Li YL, Wang SJ, Wang Q, Xing M. A comparison study on mechanical properties of polymer composites reinforced by carbon nanotubes and graphene sheet. Compos Part B-Eng. 2018;133:35-41.

[19] Zhang XC, Peng HX, Limmack AP, Scarpa F. Viscoelastic damping behaviour of cup stacked carbon nanotube modified epoxy nanocomposites with tailored interfacial condition and re-agglomeration. Composites Science and Technology. 2014;105:66-72.

[20] Sahoo NG, Rana S, Cho JW, Li L, Chan SH. Polymer nanocomposites based on functionalized carbon nanotubes. Prog Polym Sci. 2010;35(7):837-67.

[21] Dintcheva NT, Arrigo R, Morici E, Gambarotti C, Carroccio S, Cicogna F, et al. Multi-functional hindered amine light stabilizers-functionalized carbon nanotubes for advanced ultra-high molecular weight Polyethylene-based nanocomposites. Compos Part B-Eng. 2015;82:196-204.

[22] Liebscher M, Gartner T, Tzounis L, Micusik M, Potschke P, Stamm M, et al. Influence of the MWCNT surface functionalization on the thermoelectric properties of melt-mixed polycarbonate composites. Composites Science and Technology. 2014;101:133-8.

[23] Kuang YD, He XQ. Young's moduli of functionalized single-wall carbon nanotubes under tensile loading. Composites Science and Technology. 2009;69(2):169-75.

[24] Liu JQ, Xiao T, Liao K, Wu P. Interfacial design of carbon nanotube polymer composites: a hybrid system of noncovalent and covalent functionalizations. Nanotechnology. 2007;18(16).

[25] Liu L, Etika KC, Liao KS, Hess LA, Bergbreiter DE, Grunlan JC. Comparison of Covalently and Noncovalently Functionalized Carbon Nanotubes in Epoxy. Macromol Rapid Comm. 2009;30(8):627-32.

[26] Ryu J, Han M. Improvement of the mechanical and electrical properties of polyamide 6

nanocomposites by non-covalent functionalization of multi-walled carbon nanotubes. Composites Science and Technology. 2014;102:169-75.

[27] Ji XQ, Cui L, Xu YH, Liu JQ. Non-covalent interactions for synthesis of new graphene based composites. Composites Science and Technology. 2015;106:25-31.

[28] Cohen E, Dodiuk H, Ophir A, Kenig S, Barry C, Mead J. Evidences for pi-interactions between pyridine modified copolymer and carbon nanotubes and its role as a compatibilizer in poly(methyl methacrylate) composites. Composites Science and Technology. 2013;79:133-9.

[29] Zhang AB, Luan JF, Zheng YP, Sun L, Tang M. Effect of percolation on the electrical conductivity of amino molecules non-covalently coated multi-walled carbon nanotubes/epoxy composites. Appl Surf Sci. 2012;258(22):8492-7.

[30] Sanes J, Saurin N, Carrion FJ, Ojados G, Bermudez MD. Synergy between single-walled carbon nanotubes and ionic liquid in epoxy resin nanocomposites. Compos Part B-Eng. 2016;105:149-59.

[31] Vladimirov LV, Artemenko SA, Ivanov VV, Zelenetskii AN, Oleinik EF, Salamatina OB. Mechanism of reactions between epoxy compounds and amines. Polymer Science USSR. 1980;22(1):254-61.

[32] Ehlers JE, Rondan NG, Huynh LK, Pham H, Marks M, Truong TN. Theoretical study on mechanisms of the epoxy - Amine curing reaction. Macromolecules. 2007;40(12):4370-7.

[33] Wei DC, Liu YQ, Wang Y, Zhang HL, Huang LP, Yu G. Synthesis of N-Doped Graphene by Chemical Vapor Deposition and Its Electrical Properties. Nano Lett. 2009;9(5):1752-8.

[34] Ferrari AC. Raman spectroscopy of graphene and graphite: Disorder, electron-phonon coupling, doping and nonadiabatic effects. Solid State Commun. 2007;143(1-2):47-57.

[35] Wei ZJ, Pan RF, Hou YX, Yang Y, Liu YX. Graphene-supported Pd catalyst for highly

selective hydrogenation of resorcinol to 1, 3-cyclohexanedione through giant pi-conjugate interactions. Sci Rep-Uk. 2015;5.

[36] Zhang JW, Jiang DZ, Scarpa F, Peng HX. Enhancement of pullout energy in a single-walled carbon nanotube-polyethylene composite system via auxetic effect. Compos Part a-Appl S. 2013;55:188-94.

Captions

Fig. 1. Functionalization of carbon nanomaterials and the mixing of carbon nanotubes (CNTs) or graphene nanoplatelets (GNPs) with an epoxy resin: schematic diagrams showing (a) ball milling as a means of CNT or GNP functionalization, (b) the functionalization of CNTs and GNPs by melamine, and (c) the use of a planetary centrifugal mixer to blend CNT/epoxy (left) and GNP/epoxy (right) nanocomposites.

Fig. 2. Raman spectra of pristine CNTs, melamine-functionalized CNTs (M-CNTs), pristine GNPs, and melamine-functionalized GNPs (M-GNPs).

Fig. 3. Thermogravimetric analyses (TGA) of melamine, pristine CNTs, M-CNTs, pristine GNPs, and M-GNPs from room temperature to 1000°C at a heating rate of 10°C/min in air.

Fig. 4. Young's modulus and ultimate tensile strengths of pure epoxy, CNT/epoxy, M-CNT/epoxy, GNP/epoxy, and M-GNP/epoxy with 2 wt% nanofiller (n = 6~7).

Fig. 5. Scanning electron microscopy (SEM) micrographs of (a) CNT/epoxy, (b) GNP/epoxy, (c) M-CNT/epoxy, and (d) M-GNP/epoxy nanocomposites.

Fig. 6. Fracture toughness of pure epoxy, CNT/epoxy, M-CNT/epoxy, GNP/epoxy, and M-GNP/epoxy with 2 wt% nanofiller (n = 5~7).

Fig. 7. SEM micrographs of etched samples showing pull-out and crack bridging in (a) CNT/epoxy, (b) GNP/epoxy, (c) M-CNT/epoxy, and (d) M-GNP/epoxy nanocomposites. Schematic depictions of pull-out mechanisms are shown for (e) CNTs and (f) GNPs.

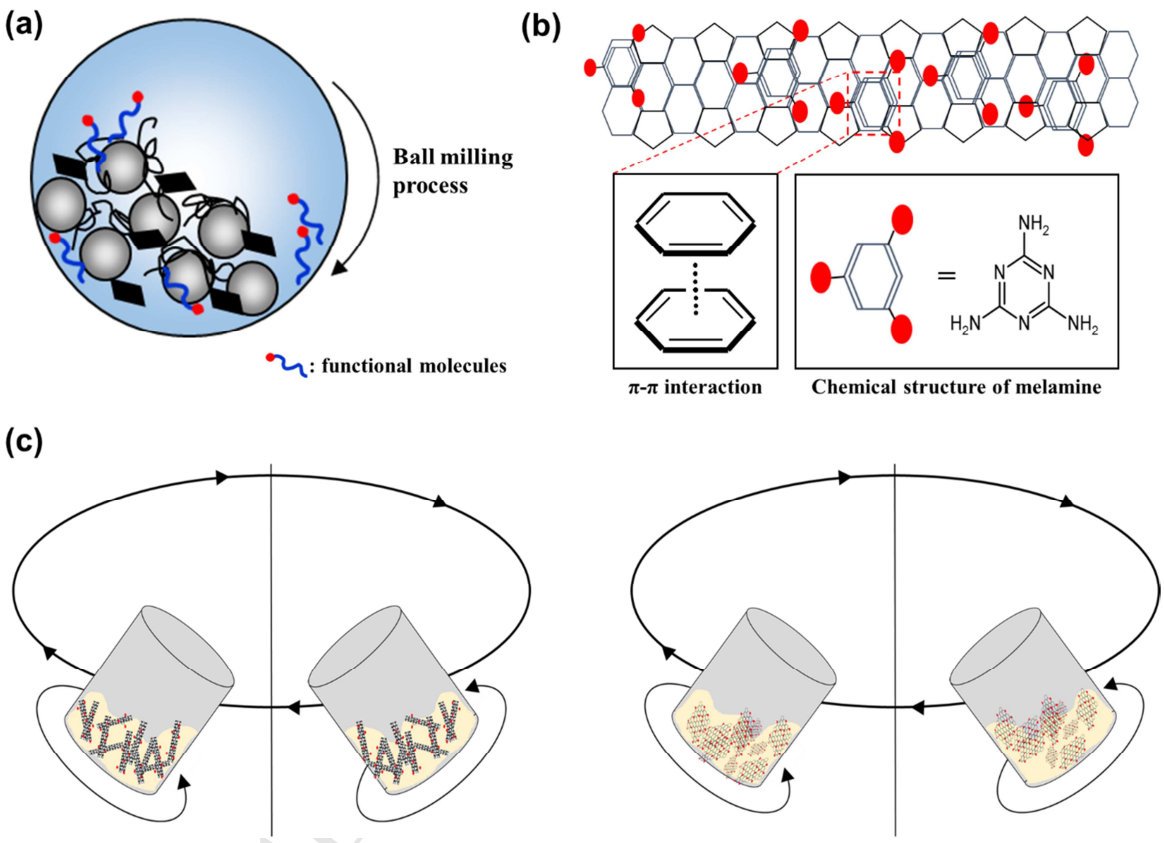

Fig. 1. Functionalization of carbon nanomaterials and the mixing of carbon nanotubes (CNTs) or graphene nanoplatelets (GNPs) with an epoxy resin: schematic diagrams showing (a) ball milling as a means of CNT or GNP functionalization, (b) the functionalization of CNTs and GNPs by melamine, and (c) the use of a planetary centrifugal mixer to blend CNT/epoxy (left) and GNP/epoxy (right) nanocomposites.

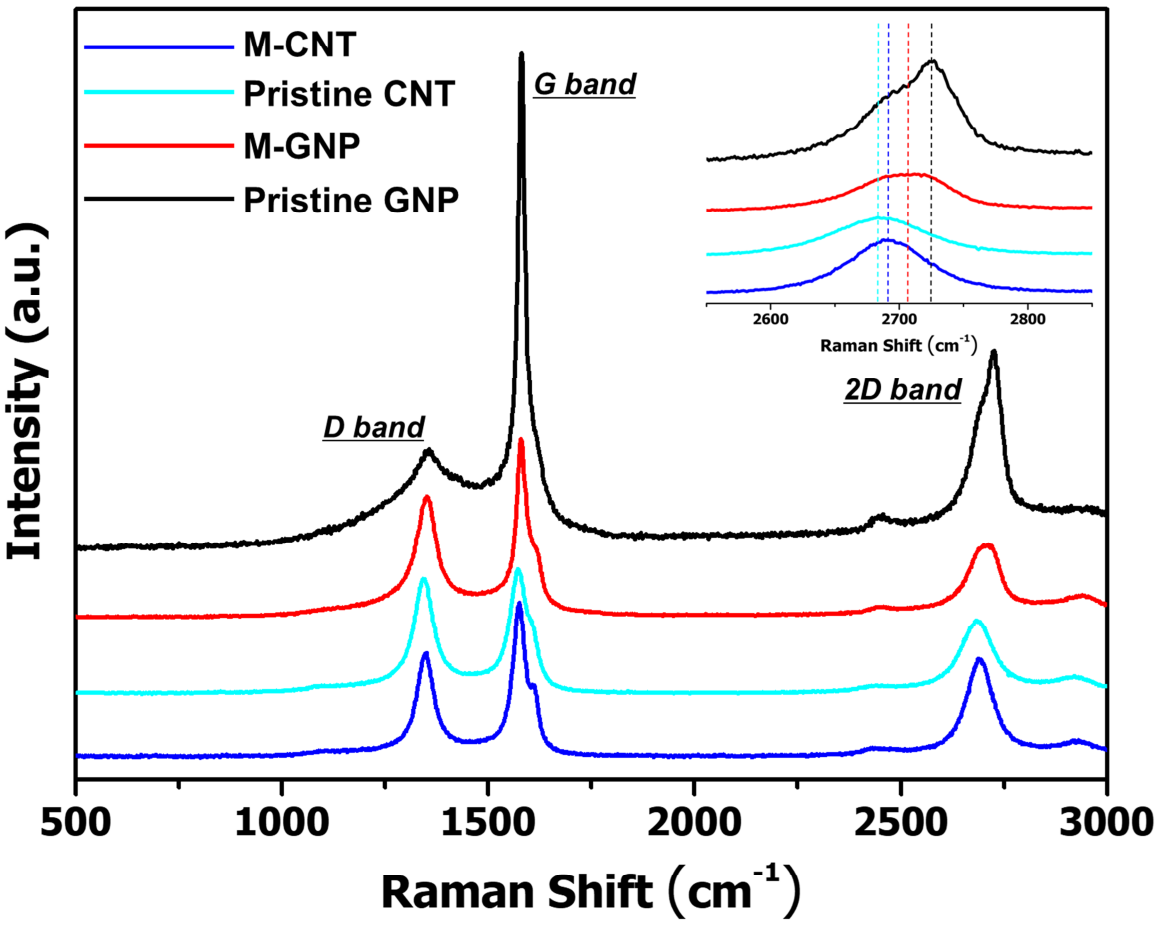

Fig. 2. Raman spectra of pristine CNTs, melamine-functionalized CNTs (M-CNTs), pristine GNPs, and melamine-functionalized GNPs (M-GNPs).

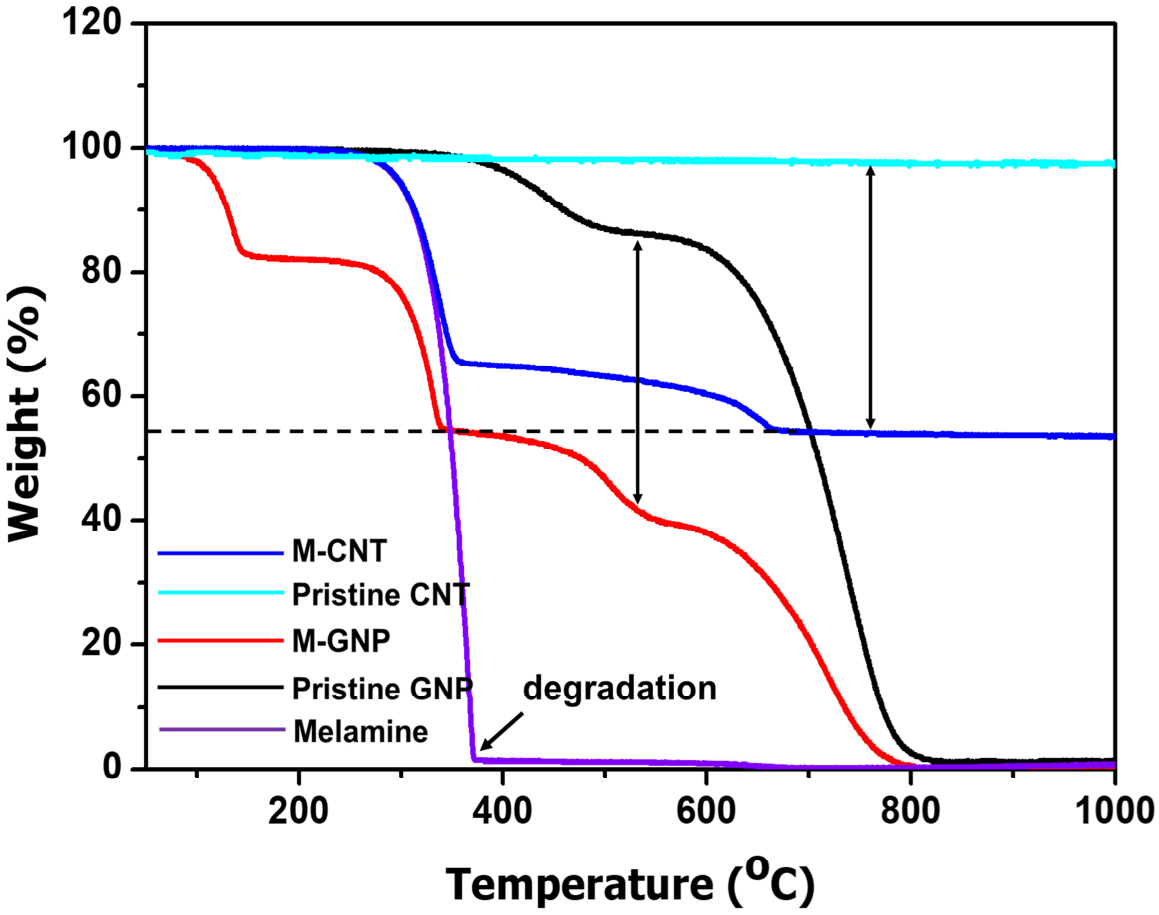

Fig. 3. Thermogravimetric analyses (TGA) of melamine, pristine CNTs, M-CNTs, pristine GNPs, and M-GNPs from room temperature to 1000°C at a heating rate of 10°C/min in air.

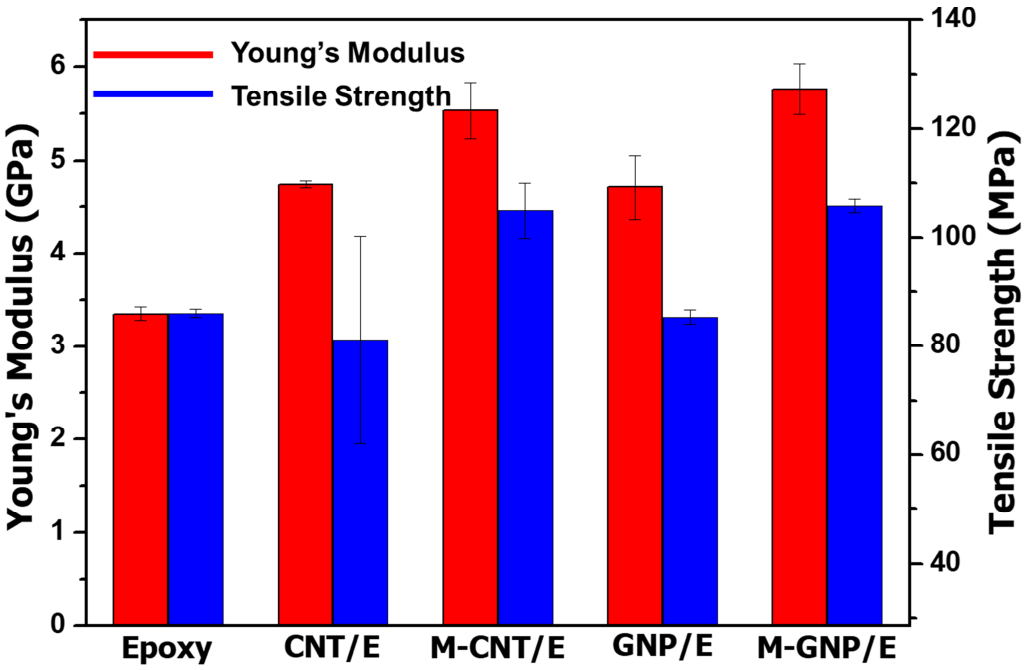

Fig. 4. Young's modulus and ultimate tensile strengths of pure epoxy, CNT/epoxy, M-CNT/epoxy, GNP/epoxy, and M-GNP/epoxy with 2 wt% nanofiller (n = 6~7).

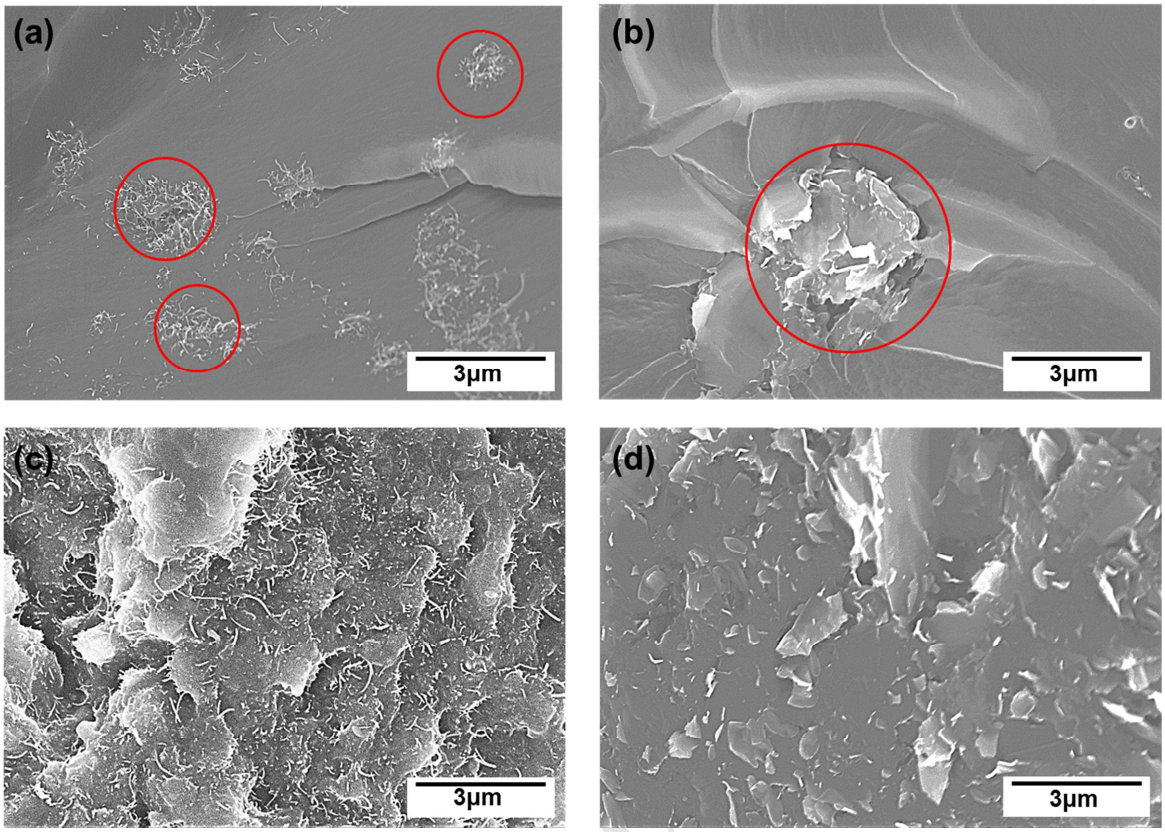

Fig. 5. Scanning electron microscopy (SEM) micrographs of (a) CNT/epoxy, (b) GNP/epoxy, (c) M-CNT/epoxy, and (d) M-GNP/epoxy nanocomposites.

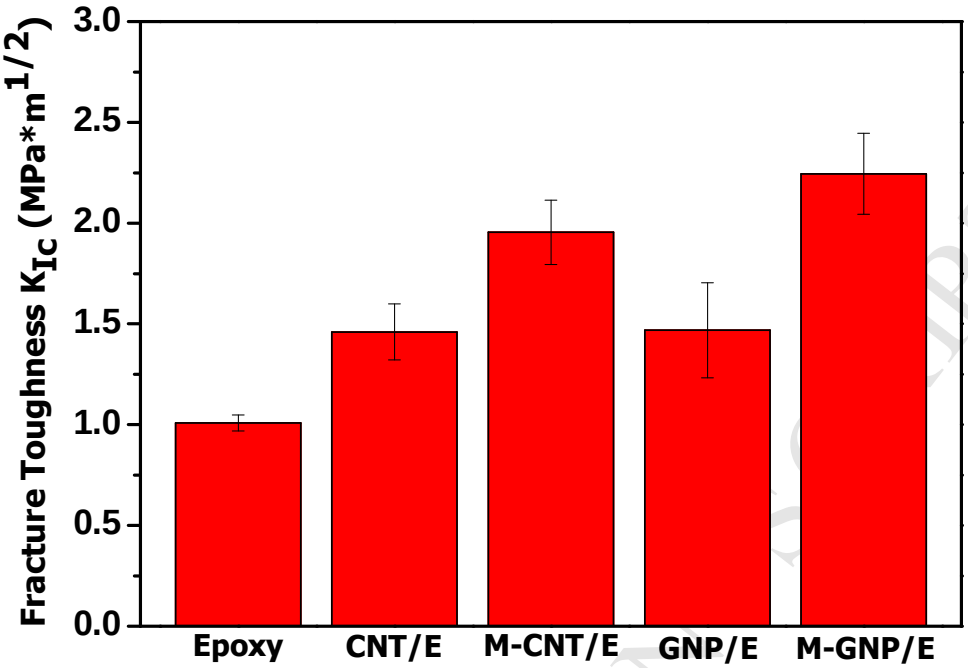

Fig. 6. Fracture toughness of pure epoxy, CNT/epoxy, M-CNT/epoxy, GNP/epoxy, and M-GNP/epoxy with 2 wt% nanofiller (n = 5~7).

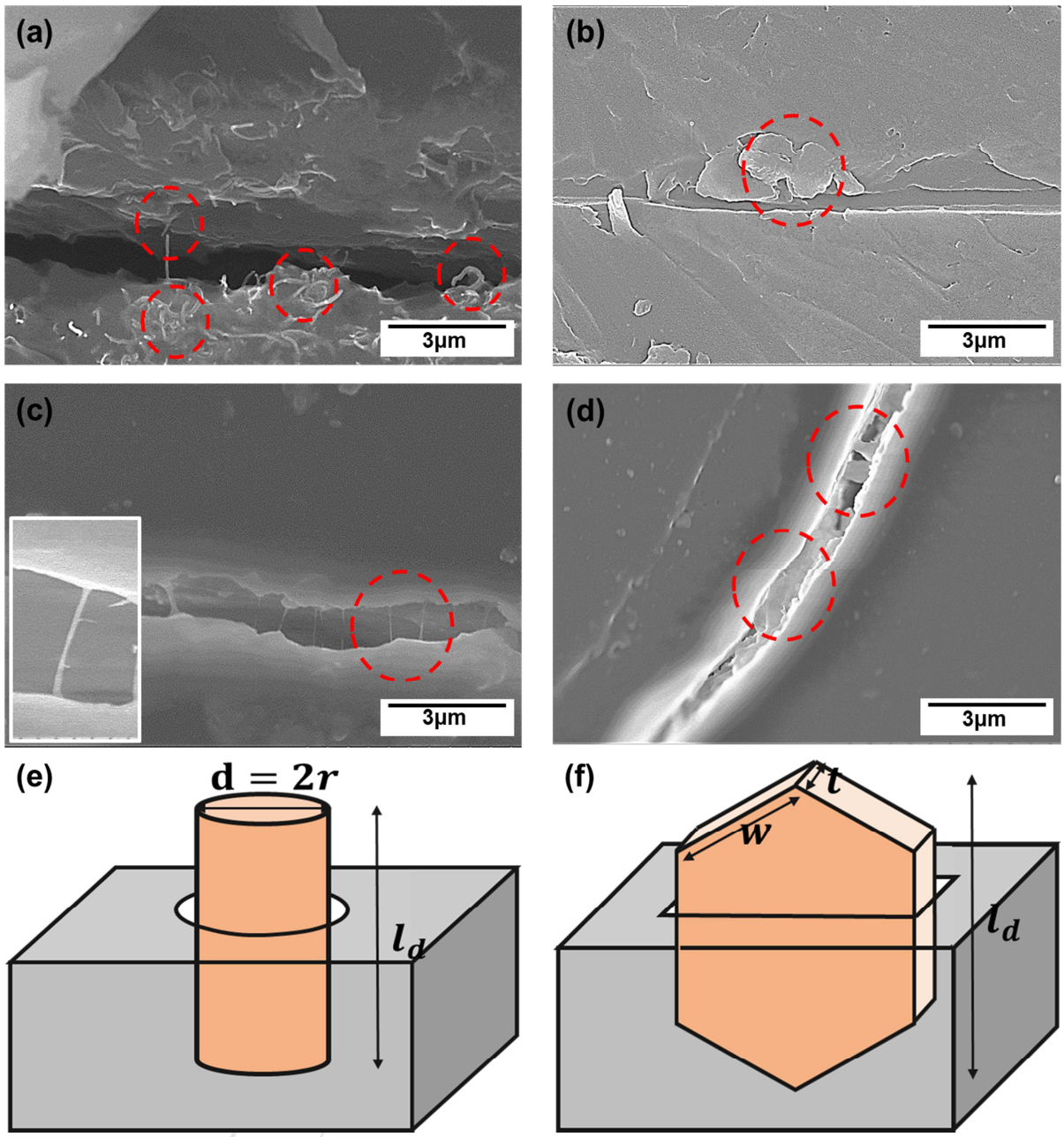

Fig. 7. SEM micrographs of etched samples showing pull-out and crack bridging in (a) CNT/epoxy, (b) GNP/epoxy, (c) M-CNT/epoxy, and (d) M-GNP/epoxy nanocomposites. Schematic depictions of pull-out mechanisms are shown for (e) CNTs and (f) GNPs.